IDE▲L®

Protein Dynamics Measurements by TROSY-Based NMR Experiments

Guang Zhu,[1] Youlin Xia, Linda K. Nicholson,* and Kong Hung Sze

Department of Biochemistry, The Hong Kong University of Science and Technology, Kowloon, Hong Kong; and
*Department of Molecular Biology and Genetics, Cornell University, Ithaca, New York 14853

The described TROSY-based experiments for investigating backbone dynamics of proteins make it possible to elucidate internal motions in large proteins via measurements of T_1, T_2, and NOE of backbone ^{15}N nuclei. In our proposed sequences, the INEPT sequence is eliminated and the PEP sequence is replaced by the ST2-PT sequence from the HSQC-based experiments. This has the benefit of shortening the pulse sequences by 5.4 ms ($=1/2J$) and results in an increase in the intrinsic sensitivity of the proposed TROSY-based experiments. The TROSY-based experiments are on average of 13% more sensitive than the corresponding HSQC-based experiments on a uniformly ^{15}N-labeled *Xenopus laevis* calcium-bound calmodulin sample on a 750-MHz spectrometer at 5°C. The amide proton linewidths of the TROSY-based experiments are 2–13 Hz narrower than those of the HSQC experiments. More sensitivity gain and higher resolution are expected if the protein sample is deuterated.   © 2000 Academic Press

Key Words: TROSY; protein dynamics; NMR; relaxation.

Complete understanding of protein function requires the detailed study of protein dynamics (*1–3*). NMR spectroscopy is a powerful tool for investigating nanosecond to picosecond and millisecond to microsecond dynamics of backbone atoms of proteins via ^{15}N relaxation studies (*4–7*). These studies include measurements of the longitudinal relaxation time (T_1) and transverse relaxation time (T_2) of backbone ^{15}N nuclei, and the heteronuclear NOE between backbone ^{15}N and the attached ^{1}H by the well-established NMR techniques based on the HSQC experiment. It is known that these techniques are less effective for NMR studies of proteins with molecular weight higher than 30 kDa. The recent development of TROSY-based NMR technology has made it possible to study larger proteins by NMR (*8*). With the proper use of the interference between dipole–dipole coupling and chemical shift anisotropy (CSA) interactions in ^{15}N–^{1}H$_N$ moieties, up to threefold sensitivity gains were obtained using TROSY-type triple resonance experiments with a 23-kDa deuterated protein when compared to the corresponding conventional experiments (*9–12*). Here, we propose TROSY-based NMR experiments for ^{15}N dynamics studies of proteins and demonstrate that the sensitivity and

linewidths obtained from the TROSY-based experiments are 13% higher and 2–13 Hz narrower than those obtained from the corresponding HSQC-based experiments on a 750-MHz Varian Inova spectrometer at 5°C on a uniformly ^{15}N-labeled *Xenopus laevis* calcium-bound calmodulin sample. More sensitivity gain and higher resolution are expected when a deuterated protein sample is used. The described methods should allow investigation of protein dynamics beyond the limitations of commonly used NMR techniques.

The pulse sequences based on TROSY for measuring T_1, T_2, and NOE of ^{15}N–^{1}H$_N$ moieties are depicted in Fig. 1A (T1-TROSY), Fig. 1B (T2-TROSY), and Fig. 1C (NOE-TROSY), respectively. In earlier pulse sequences for ^{15}N relaxation studies (*13*), a reverse half-INEPT sequence was used to produce the required antiphase magnetization of ^{15}N before the PEP (preservation of equivalent path) sequence (*14*). In our proposed sequences, this INEPT sequence is eliminated and the PEP sequence is replaced by the ST2-PT (single transition to single transition polarization transfer) sequence (*9, 15*). The introduction of TROSY components in this way not only effectively selects the slowest relaxing component of the ^{15}N–^{1}H moiety, but also has the benefit of shortening the pulse sequences by 5.4 ms ($=1/2J$) and results in a great increase in sensitivity, while the resultant analysis of the protein dynamics remains unchanged with respect to the conventional HSQC-based relaxation experiments.

In the T1-TROSY and T2-TROSY pulse sequences (Figs. 1A and 1B), the first 90° pulse of ^{15}N and the subsequent gradient g1 are used to remove the steady-state magnetization of ^{15}N to ensure that magnetization originates solely from ^{1}H and not from ^{15}N (*13*). The ^{1}H 180° selective pulses in the T1-TROSY T period (Fig. 1A), which minimally perturb water magnetization, are applied every 5–10 ms in order to suppress the effects of ^{1}H–^{15}N dipolar and CSA cross correlation. In the modified CPMG section of the T2-TROSY pulse sequence (Fig. 1B), ^{1}H 180° pulses are inserted every 5–10 ms to invert the ^{1}H spin state rapidly in order to average the relaxation rates of the multiplet components (*4–7, 16*). In the latest version of the NOE pulse sequence proposed by Farrow *et al.* (*13*), the first 90° ^{1}H pulse and its flanking gradients g1 and g2 of its predecessor sequence are removed, since only in-phase ^{15}N
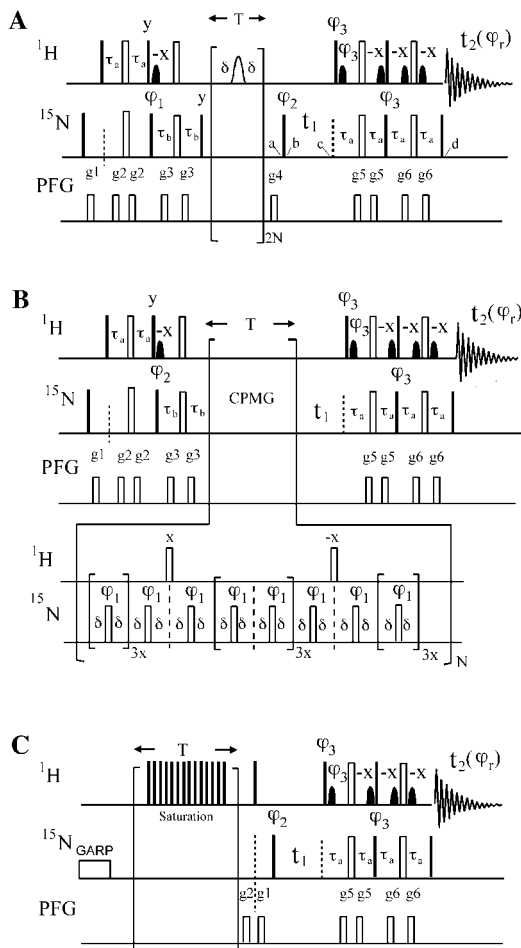
FIG. 1. Pulse sequences for the measurement of (A) ^{15}N T_1 (T1-TROSY), (B) ^{15}N T_2 (T2-TROSY), and (C) ^{1}H–^{15}N NOE (NOE-TROSY). In all sequences, filled bars and open bars represent 90° and 180° pulses, respectively. Filled shaped pulses are 1.1-ms sinc-modulated rectangular 90° pulses to selectively excite the water resonance. Default phases are x, $\tau_a = 2.25$ ms and $\tau_b = 1/(4\,^1J_{\rm NH}) \approx 2.75$ ms. For all three experiments, echo/antiecho selections during t_1 were made by reversing φ_3 and the even number phases of the receiver. In order to remove axial peaks in the ω_1 dimension, phase φ_2 and the receiver phase $\varphi_{\rm r}$ were inverted for every second t_1 increment. The durations and strengths of the gradients are g1 = (0.4 ms, 15 G/cm); g2 = (0.4 ms, 8 G/cm); g3 = (0.4 ms, 15 G/cm); g4 = (1 ms, 10 G/cm); g5 = (0.5 ms, 5 G/cm); g6 = (0.4 ms, 15 G/cm). In the T1-TROSY sequence (A), an even number of shaped pulses, 333-μs cosine-modulated rectangular 180° pulses with excitation maximum positioned at 4 ppm downfield from the carrier (on water), are applied every 5 ms ($\delta = 2.5$ ms) during recovery time T. Experimental recovery delay is 1.1 s. Phase cycling is as follow: $\varphi_1 = 4(x)$, $4(-x)$; $\varphi_2 = (y, x, -y, -x)$; $\varphi_3 = (y)$; $\varphi_{\rm r} = (x, -y, -x, y, -x, y, x, -y)$. In T2-TROSY (B), $\delta = 0.55$ ms, experimental recovery delay is 2 s. In order to reduce heating during the CPMG portion, the ^{15}N pulse power is decreased by 6 dB compared with that in (B) and (C). Phase cycling: $\varphi_1 = (y, x)$; $\varphi_2 = (y, -x, -y, x)$; $\varphi_3 = (y)$; $\varphi_{\rm r} = (x, -y, -x, y)$. In NOE-TROSY (C), ^{1}H saturation is achieved by the application of 120° pulses spaced at 5-ms intervals for 3 s prior to the first ^{15}N pulse. An overall delay between scans of 5 s was employed in both the NOE and the NONOE experiments. Phase cycling used is $\varphi_2 = (y, x, -y, -x)$; $\varphi_3 = (y)$; $\varphi_{\rm r} = (x, -y, -x, y)$. The duration and power of GARP decoupling on ^{15}N channel are 100 ms and 3.5 kHz, respectively.

polarization (S_z) before the first 90° ^{15}N pulse can be transferred to the observable signal, whereas the steady-state magnetization (I_z) of ^{1}H does not contribute to the detectable signal. In the described NOE-TROSY pulse sequence (Fig. 1C), the first 90° ^{1}H pulse and its flanking gradients g1 and g2 are necessary to remove the steady-state magnetization of ^{1}H because both the in-phase polarization (S_z) and the antiphase polarization ($2S_zI_z$) of ^{15}N before the first 90° ^{15}N pulse can be transferred to the observable magnetization. In principle, the steady-state ^{15}N magnetization can be removed by a 90° ^{15}N pulse and flanking gradients. However, it was found that full removal required an additional ^{15}N GARP decoupling sequence applied after the acquisition period in our pulse sequence. The use of postacquisition decoupling also generates the same heating effect as the decoupling field applied during acquisition in the HSQC-based experiments and makes comparison of the two approaches easier (see supplementary material, available from the authors).

Evolution of the density operator in the T1-TROSY pulse sequence at different time points (Fig. 1A) can be described as

$$\sigma_a = S_z.$$

For the first two scans, with $\varphi_1 = x$, $\varphi_2 = (y, x)$, $\varphi_3 = y$, $\varphi_{\rm r} = (x, -y)$,

$$\sigma_b = S_- = S_-I_\alpha + S_-I_\beta \xrightarrow{\;t_1\;} \sigma_c$$

$$= S_-I_\alpha e^{i(\omega_S + \pi J)t_1} + S_-I_\beta e^{i(\omega_S - \pi J)t_1},$$

where S and I are spin operators of ^{15}N and ^{1}H, respectively, $S_\pm = S_x \pm iS_y$, $I_\pm = I_x \pm iI_y$, $S_{\alpha,\beta} = 0.5E \pm S_z$, $I_{\alpha,\beta} = 0.5E \pm I_z$, and E is the identity matrix. S_α and S_β correspond to the $|\alpha\rangle$ and $|\beta\rangle$ spin states of the S spin, respectively, while I_α and I_β correspond to the $|\alpha\rangle$ and $|\beta\rangle$ spin states of the I spin, respectively. The detected magnetization after the ST2-PT section can be expressed as

$$\sigma_d = iI_-S_\beta e^{-i(\omega_S + \pi J)t_1} e^{i(\omega_I - \pi J)t_2},$$

where the term I_+S_α is omitted because it cannot be detected. Another transient can be acquired as

$$\sigma_d = iI_-S_\beta e^{i(\omega_S + \pi J)t_1} e^{i(\omega_I - \pi J)t_2},$$

with $\varphi_1 = x$, $\varphi_2 = (y, x)$, $\varphi_3 = -y$, $\varphi_{\rm r} = (x, y)$ as stated in the legend to Fig. 1. The real part of the FID can be obtained by adding the above two transients, while the imaginary part of the FID is obtained by subtracting the above two transients and then performing a 90° phase shift (*17, 18*). Analyses for the
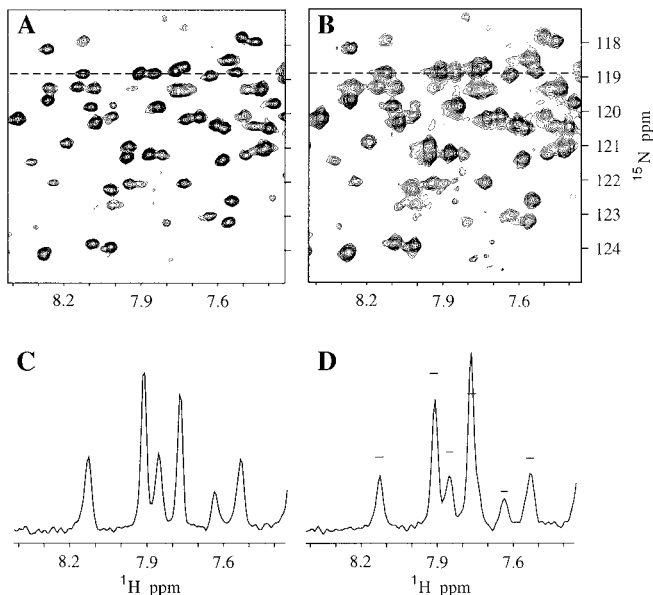
FIG. 2. Sections of T1-TROSY spectrum (A) and the corresponding T1-HSQC spectrum (B) of protein calmodulin recorded on a Varian Inova 750-MHz spectrometer at 5°C. Both spectral sections are recorded and processed with the same parameters. They are plotted at the same levels with contour spacing being 1.2. For the convenience of comparison, the spectrum (A) is shifted 45 Hz in both ^{1}H and ^{15}N dimensions. (C) and (D) are the 1D slices taken from spectra (A) and (B), respectively, at the dotted line positions. The short bars in spectrum (D) mark the heights of the corresponding peaks in (C).

other two proposed sequences can be carried out in a similar manner.

To demonstrate the effectiveness of the proposed experiments, we first simulated a large protein by performing the TROSY- and HSQC-based experiments on a 17-kDa protein at low temperature. We compared the sensitivity and linewidths of two spectra obtained by T1-TROSY and its corresponding HSQC experiment acquired for a uniformly ^{15}N-labeled *X. laevis* calcium-bound calmodulin sample (1.0 mM in 0.1 mM KCl, 6.8 mM CaCl$_2$, pH 6.5, 90% H$_2$O/10% D$_2$O) at 5°C on a Varian Inova 750-MHz NMR spectrometer with the relaxation delay $T = 10.7$ ms. The sections of the 2D spectra are displayed in Figs. 2A and 2B corresponding to the same regions of the spectra recorded by T1-TROSY and T1-HSQC experiments. It was shown that the peaks in the T1-TROSY spectrum were on average 13% more intense and 2–14 Hz narrower than the corresponding peaks in the T1-HSQC spectrum, when 80 isolated peaks were selected for comparison.

To compare the dynamic parameters obtained from the conventional HSQC (*13*) and the proposed TROSY methods, the corresponding two sets of spectra were recorded. In all experiments, 256* × 1024* (* expresses complex points) $t_1 \times t_2$ data matrices in the time domain were acquired with spectral widths of 3000 and 10,500 Hz, respectively. The T_1 values were measured from spectra recorded with eight different relaxation delays with $T = 10.7$, 85.3, 192.0, 320.0, 480.0,

693.3, 981.3, and 1440.0 ms. The T_2 values were determined from spectra recorded with relaxation delays $T = 19.4$, 38.8, 58.3, 77.7, 97.1, 136.0, 174.8, and 213.7 ms. The NOE values were determined from spectra recorded in the presence (NOE) and absence (NONOE) of a proton presaturation period of 3 s. The numbers of scans were 16, 16, and 64 for T_1, T_2, and NOE experiments, respectively. All data processing was performed using the nmrPipe software package (*19*). All spectral matrices were 4096 × 4096 with identical processing parameters. The temperature used for this comparison was at 35°C so that TROSY-based experiments and the corresponding HSQC experiments have enough sensitivity to allow easier comparison.

In order to evaluate the significance of the small differences between relaxation parameters obtained by TROSY-based experiments and HSQC-based experiments, a statistical analysis utilizing Student's t test (*20, 21*) was carried out between corresponding T_1, T_2, and NOE data sets. The calculated significance probabilities were 0.83, 0.82, and 0.73 for T_1, T_2, and NOE data, respectively. Compared with a critical probability of 0.05 for the 95% confidence level, these values clearly indicate that the measured relaxation parameters by TROSY-based experiments are not significantly different from those obtained by HSQC-based experiments. From a statistical analysis of the pairwise differences between relaxation values obtained with the two methods, the following (mean, standard deviations, maximum, minimum) values of (0.00, 0.01, 0.03, −0.03), (−0.002, 0.002, 0.001, −0.007), and (−0.01, 0.05, 0.07, −0.10) were obtained for T_1, T_2, and NOE data, respectively. It should be noted that, even for extreme cases where the pairwise differences are either at maximum or minimum, the deviations are not statistically significant at the 99% confidence level when compared with the root-mean-squared standard deviations in the corresponding measurements. Hence, it is shown that an excellent agreement between the TROSY-based experiments and the corresponding HSQC-based experiments is obtained.

It is also shown in the presented studies that the proposed TROSY experiments are only about 5% less sensitive (rather than the 50% expected based on observation of a single component of the multiplets) at 35°C than the corresponding HSQC experiments under the experimental conditions described above. This sensitivity gain is due to the following facts. First, due to the TROSY effect, the cross-peaks in the TROSY-based spectra are 3–5 Hz narrower in linewidths in both dimensions when compared with the linewidths of corresponding cross-peaks in the HSQC-based spectra. Second, in the proposed TROSY-based pulse sequences, the time during which magnetization resides in the transverse plane is 5.4 ms shorter than that in the corresponding HSQC pulse sequences, resulting in great sensitivity gain. These effects are clearly demonstrated in Figs. 2A–2D, where the T1-TROSY and T1-HSQC experiments were recorded with calmodulin at 5°C, a temperature at which calmodulin tumbles at an estimated rate

of 16 ns assuming isotropic tumbling. This is equivalent to the tumbling rate of a 40- to 50-kDa protein at room temperature. The sensitivity gain will be more pronounced when larger and deuterated biomolecules (>30 kDa) are employed in these NMR relaxation studies.

In summary, the described TROSY-based experiments for protein dynamics studies represent a significant advancement in the ability to elucidate internal motions in large proteins. It is demonstrated that even for the ^{15}N-labeled protein calmodulin, the TROSY-based experiments yield spectral linewidths that are 2–13 Hz more narrow and sensitivity that is 13% higher than those obtained from the corresponding HSQC experiments at 5°C on a 750-MHz NMR spectrometer. Even at 35°C, the sensitivity of the TROSY-based experiments is comparable to that of the HSQC experiments, but with higher resolution (linewidths are 3–5 Hz more narrow than those of the HSQC experiments). The proposed experiments will allow characterization of the dynamics of proteins with molecular weight in excess of 30 kDa. In particular, these techniques open new possibilities for the study of multiprotein complexes in which a single subunit can be isotopically labeled, eliminating much of the spectral overlap problem. In conjunction with newly developed TROSY-based triple resonance experiments for backbone resonance assignments, the proposed relaxation experiments offer a powerful approach for furthering our understanding of the dynamic nature of proteins.

SUPPLEMENTARY MATERIALS

The supplementary material consists of a figure showing T_1 and T_2 fits and a table showing T_1, T_2, and NOE measured by the TROSY-based experiments and the corresponding HSQC experiments for isolated peaks and is available from the authors.

ACKNOWLEDGMENTS

REFERENCES

1. A. Amadei, A. B. M. Linssen, and H. J. C. Berendsen, *Proteins* **17,** 412–425 (1993).

2. V. A. Feher and J. Cavanagh, *Nature* **400,** 289–293 (1999).

3. M. Karplus and G. A. Petsko, *Nature* **347,** 631–639 (1990).

4. G. Barbato, M. Ikura, L. E. Kay, R. W. Pastor, and A. Bax, *Biochemistry* **31,** 5269–5278 (1992).

5. L. E. Kay, D. A. Torchia, and A. Bax, *Biochemistry* **28,** 8972–8979 (1989).

6. L. E. Kay, L. K. Nicholson, F. Delaglio, A. Bax, and D. A. Torchia, *J. Magn. Reson.* **97,** 359–375 (1992).

7. M. V. Milburn, L. Tong, A. M. De Vos, A. Brunger, Z. Yamaizumi, S. Nishimura, and S-H. Kim, *Science* **247,** 939–945 (1990).

8. K. Pervushin, R. Riek, G. Wider, and K. Wüthrich, *Proc. Natl. Acad. Sci. USA* **94,** 12366–12371 (1997).

9. M. Salzmann, K. Pervushin, G. Wider, H. Senn, and K. Wüthrich, *Proc. Natl. Acad. Sci. USA* **95,** 13585–13590 (1998).

10. M. Salzmann, G. Wider, K. Pervushin, H. Senn, and K. Wüthrich, *J. Am. Chem. Soc.* **121,** 844–848 (1999).

11. M. Salzmann, K. Pervushin, G. Wider, H. Senn, and K. Wüthrich, *J. Biomol. NMR* **14,** 85–88 (1999).

12. D. Yang and L. E. Kay, *J. Biomol. NMR* **13,** 3–10 (1999).

13. N. A. Farrow, R. Muhandiram, A. U. Singer, S. M. Pascal, C. M. Kay, G. Gish, S. E. Shoelson, T. Pawson, J. D. Forman-Kay, and L. E. Kay, *Biochemistry* **33,** 5984–6003 (1994).

14. J. Cavanagh and M. Rance, *Annu. Rep. NMR Spectrosc.* **27,** 1–58 (1993).

15. K. Pervushin, R. Rie, G. Wider, and K. Wüthrich, *J. Am. Chem. Soc.* **120,** 6394–6400 (1998).

16. A. G. Palmer III, J. Skelton, W. J. Chazin, P. E. Wright, and M. Rance, *Mol. Phys.* **75,** 699–711 (1992).

17. G. Zhu, X. M. Kong, X. Z. Yan, and K. H. Sze, *Angew. Chem. Int. Ed. Engl.* **37,** 2859–2861 (1998).

18. G. Zhu, X. M. Kong, and K. H. Sze, *J. Biomol. NMR* **13,** 77–81 (1999).

19. F. Delaglio, S. Grzesiek, G. W. Vuister, G. Zhu, J. Pfeifer, and A. Bax, *J. Biomol. NMR* **6,** 277–293 (1995).

20. W. H. Press, S. A. Teukilsky, W. T. Vettering, and B. P. Flannery, "Numerical Recipes in C," 2nd ed., Cambridge Univ. Press, Cambridge, UK (1992).

21. R. R. Sokal and F. J. Rohlf, "Biometry: The Principles and Practice of Statistics in Biological Research," 2nd ed., Freeman, New York (1995).